

# Improving apple fruit firmness predictions by effective correction of multispectral scattering images<sup>☆</sup>

Yankun Peng<sup>a,\*</sup>, Renfu Lu<sup>b</sup>

<sup>a</sup> Department of Biosystems and Agricultural Engineering, Michigan State University, 127 Farrall Hall, East Lansing, MI 48824, USA

<sup>b</sup> USDA Agricultural Research Service, Michigan State University, 224 Farrall Hall, East Lansing, MI 48824, USA

Received 5 December 2005; accepted 18 April 2006

## Abstract

Firmness is an important parameter in determining the maturity and quality grade of apple fruit. The objective of this research was to improve the multispectral imaging system used in our previous studies and refine scattering analysis methods for more effectively measuring apple fruit firmness. An improved multispectral imaging system equipped with a light intensity controller was used to measure light scattering from ‘Red Delicious’ apples at seven wavelengths and ‘Golden Delicious’ apples at eight wavelengths. A correction method was proposed to reduce noise signals in the scattering images during radial averaging of image pixels. Apple shape/size affected scattering intensity and distance, and two methods were proposed for correcting their effects. The corrected scattering images were reduced to spatially symmetrical profiles by radial averaging. A modified Lorentzian distribution (MLD) function with four parameters was used to fit the scattering profiles. Firmness prediction models were developed by multi-linear regression against MLD parameters for two apple cultivars. The improved system yielded better firmness predictions with the correlation ( $r$ ) of 0.898 and the standard error of validation (S.E.V.) of 6.41 N for ‘Red Delicious’ apples and  $r=0.897$  and S.E.V.=6.14 N for ‘Golden Delicious’ apples.

© 2006 Elsevier B.V. All rights reserved.

**Keywords:** Fruit; Apples; Firmness; Multispectral imaging; Scattering; Lorentzian function

## 1. Introduction

Firmness is a key parameter in the grading standards for shipping, marketing, storing, and processing apples. Firmness is also an important parameter in determining apple maturity and harvest time. The firmness of apple fruit varies during the growth and maturation period dependent on cultivar, climate, season, and cultural practice. Apple firmness is commonly measured with the Magness–Taylor (MT) firmness tester, which requires the penetration of a mechanical probe into the fruit for a specified depth. Because of its destructive nature, MT measurement is only suitable for sampling purposes and cannot be used for grading or sorting fruit.

Considerable research has been reported on non-destructive measurement of fruit firmness for apples and other fresh fruit by mechanical methods including quasi-static and dynamic force/deformation, impact, and sonic (Delwiche et al., 1987; Meredith et al., 1990; Delwiche and Sarig, 1991; Zhang et al., 1994; Chen and Tjan, 1996; Galili et al., 1998; Ozer et al., 1998; Stone et al., 1998; Sugiyama et al., 1998; McGlone et al., 1999; Ruiz-Altisent and Ortiz-Canavate, 2005). These mechanical methods appear promising, but their relationship with the standard destructive method has not been consistent for firm fruit such as apples (Shmulevich et al., 2003; Lu, 2004). The fruit industry and horticulturists are still reluctant to accept these non-destructive firmness methods as a viable alternative to replace the MT firmness tester.

Research has been reported on using alternative optical means such as near-infrared spectroscopy (NIRS) to measure fruit firmness, but the correlation with MT measurement is low and the results are unsatisfactory (McGlone and Kawano,

<sup>☆</sup> Mention of commercial products is only for providing factual information for the reader and does not imply endorsement by the United States Department of Agriculture.

\* Corresponding author. Tel.: +1 517 353 5270; fax: +1 517 432 2892.

E-mail address: [pengy@msu.edu](mailto:pengy@msu.edu) (Y. Peng).

1998; Lu et al., 2000; Lu and Ariana, 2002). Researchers also have studied light scattering as a means for measuring fruit quality including firmness. McGlone et al. (1997) used a single-channel charge coupled device (CCD) detector to measure light scattering from kiwifruit generated by a laser at 864 nm. However, scattering at single wavelengths is not sufficient for accurate prediction of fruit firmness.

Lu (2003, 2004) proposed a new method of measuring scattering images from fruit at multiple wavelengths in the visible and near-infrared (NIR) region for estimating fruit firmness. A neural network model was developed with the inputs of radial scattering profiles to predict fruit firmness, which gave the correlation coefficient ( $r$ ) of 0.87 and the standard error for validation (S.E.V.) of 5.90 N when four wavelengths were used. Peng and Lu (2005) proposed a Lorentzian distribution (LD) function with three parameters to characterize the scattering profiles of multispectral scattering images. Later, Peng and Lu (2006a,b) proposed a modified Lorentzian distribution (MLD) function with four parameters to describe the entire scattering profiles, including saturation area, of spectral scattering images acquired from a compact multispectral imaging system with a liquid crystal tunable filter (LCTF). Using this LCTF-based multispectral imaging system, an optimal set of wavelengths between 650 and 1000 nm was determined for predicting apple fruit firmness. A linear prediction model was developed to describe the relationship between the MT firmness of 'Red Delicious' apples and their MLD parameters at seven wavelengths with  $r = 0.82$  and S.E.V. = 6.64 N. In these studies the multispectral scattering images were not corrected for the potential effect of noise signals resulting from the existence of abnormal fruit tissue (i.e. isolated dark or bright spots on the fruit surface) and the surface of apples was considered to be a plane in radial averaging.

This paper reports on firmness prediction results from an improved multispectral scattering technique. Specific objectives of this research were to: (1) increase the stability of the light source; (2) reduce the negative influence of noise signals in multispectral scattering images caused by isolated abnormal (dark or bright) spots on the fruit to enhance apple firmness predictions; (3) incorporate the effect of apple size/shape into the calculations of scattering intensity and distance for more accurate description of scattering profiles; (4) verify the effectiveness of the improved multispectral imaging system by assessing the firmness of two cultivars of apple fruit.

## 2. Materials and methods

### 2.1. Apple samples

Two apple cultivars, 572 'Red Delicious' (RD: *M. pumila*) and 547 'Golden Delicious' (GD: *M. pumila*) apple samples were used for experiments. They were harvested from orchards at Michigan State University (MSU) Clarksville

Horticultural Experiment Station in Clarksville, Michigan and MSU Horticultural Teaching and Research Center in East Lansing, Michigan during the harvest season in 2004. The apples were stored in either controlled atmosphere environment (2% O<sub>2</sub> and 3% CO<sub>2</sub> at 0 °C) or refrigerated air (0 °C) prior to testing. The apple samples were placed at room temperature (21 °C) for at least 15 h before experiments were started. The experiments were carried out over a 1-week period. Approximately 100 samples were measured for a given test day. The statistics of fruit firmness for all test apple samples are: mean firmness = 58.12 N for RD and 50.79 N for GD; the standard deviation (S.D.) = 14.56 N for RD and 13.44 N for GD; minimum firmness = 21.17 N for RD and 25.06 N for GD; and maximum firmness = 99.24 N for RD and 81.51 N for GD. The size of apple samples was between 69.80 and 82.60 mm in the equatorial diameter.

### 2.2. Multispectral imaging system

Fig. 1 shows a compact laboratory multispectral imaging system, which was improved over our previous system (Peng and Lu, 2006a,b). This system mainly consisted of an NIR enhanced CCD camera (UM-300, UNIQ, CA, USA), a liquid crystal tunable filter (LCTF: VariSpec Standard Tunable Filter, CRI, MA, USA) ranging between 650 and 1100 nm, a 250 W quartz tungsten halogen lamp light source equipped with a DC control unit (Thermo Oriel, Stratford, CT, USA), a light intensity controller (Model 68950, Spectra-Physics, CT, USA) that was newly installed, and a computer for controlling and managing the whole system. The multispectral imaging system was enclosed in a black imaging chamber to shield it from ambient light. The beam size was 1.5 mm and the camera exposure time was set at 1.2 s for all the samples. With this beam size and exposure time, we were able to obtain scattering images from an area of 30 mm diameter around the equator of the fruit. The wavelength of LCTF was selected or tuned between 650 and 1000 nm via the computer during the acquisition of scattering images. A commercial application program (XCAP, Epix Inc., IL, USA) was utilized to control the imaging system, capture scattering images from samples, and save the images in the computer.

The light source supplier is highly regulated to operate the lamp at constant current, even if the line voltage changes. However, even with the lamp current being constant, the light output of the lamp still varies resulting from the lamp aging, filament or electrode erosion, gas adsorption or desorption, and ambient temperature. These effects cause changes in the spectral intensity and spectral power distribution. The light intensity controller corrects for the lamp output changes, maintaining a constant short and long-term output from the lamp. The light output regulating unit is made up of a light sensing head and a controller. The silicon-based light sensor monitors part of the light source output; the controller constantly compares the recorded signal to the preset level and changes the power supply output to keep the measured signal at the set level.

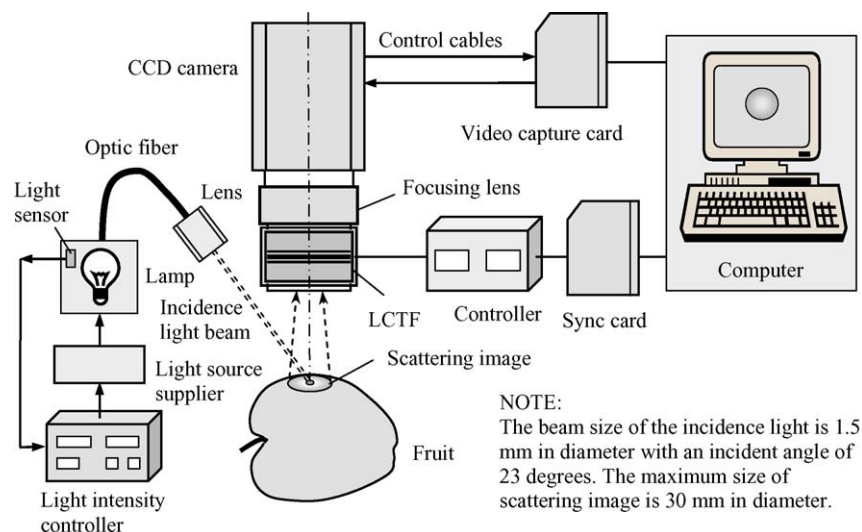


Fig. 1. Schematic of the multispectral imaging system for acquiring spectral scattering images from fruit.

### 2.3. Experimental procedure

Each fruit, after being cleaned with cloth, was placed between the horizontal holder with a round hole of 30 mm diameter and a spring support beneath the holder. The imaging system captured spectral scattering images from the equator of each fruit at a spatial resolution of 0.1 mm/pixel. A total of seven images were acquired for each RD apple sample at seven wavelengths (680, 700 nm, 740, 800, 820, 910, and 990 nm). These wavelengths were selected on the basis of the optimal wavelengths determined in our previous study (Peng and Lu, 2006a,b). Similarly, for each GD apple, spectral scattering images were acquired at eight wavelengths (650, 680, 700, 740, 820 nm, 880, 910, and 990 nm). A typical raw scattering image acquired from a GD apple is shown in Fig. 2(a).

The MT firmness test was performed immediately after the imaging of all apples. A portion of fruit skin (about 1–2 mm thick) was removed from the same imaging area of each apple fruit. MT firmness was measured from the peeled area using an 11-mm MT probe mounted on a Texture Analyzer (Stable Micro Systems, Surrey, UK) at a loading speed of 2 mm/s. Maximum force recorded during the 9 mm penetration of the fruit tissue was used as a reference measure of fruit firmness.

### 2.4. Data analysis methods

The scattering images were radially symmetric with respect to the light incident point as shown Fig. 2(a), and their intensity decreased rapidly as the distance from the light incident point increased. To obtain one-dimensional scattering profiles, the beam incident center was first identified for each scattering image by the center of weighted gravity method (Weeks, 1996; Lu, 2004) and the scattering image was then divided into 150 concentric circles with an equal distance (circular bandwidth = 1 pixel  $\times$  0.10 mm/pixel = 0.10 mm). The radial intensity (CCD grayscale) of each circular band was

calculated by averaging all pixels within the band to obtain radial scattering profiles. After radial averaging, each scattering profile was represented by 150 data points covering the 30 mm diameter area. Fig. 2(b) shows a one-dimensional scattering profile obtained from the scattering image shown

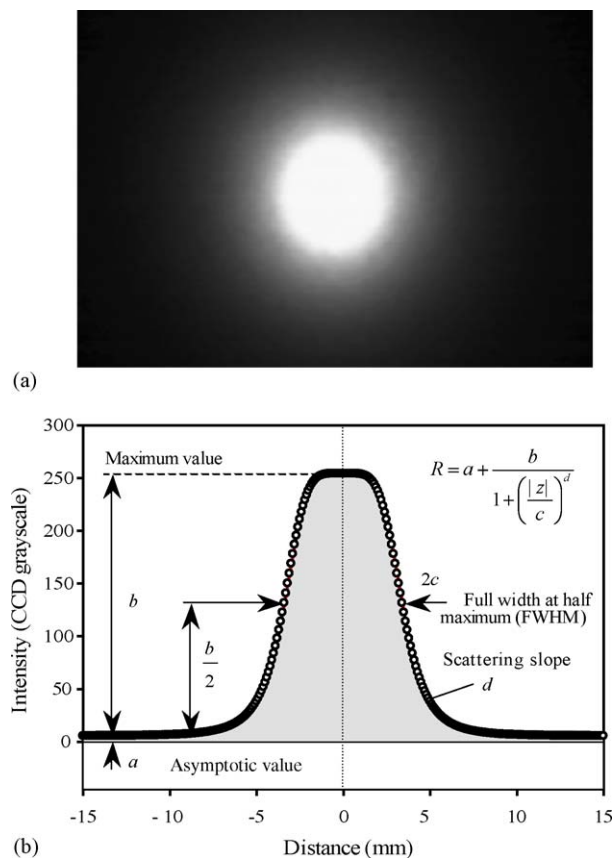


Fig. 2. A profile of the radial scattering image: (a) a raw scattering image obtained from a 'Golden Delicious' apple; (b) a scattering profile described by a modified Lorentzian distribution model.

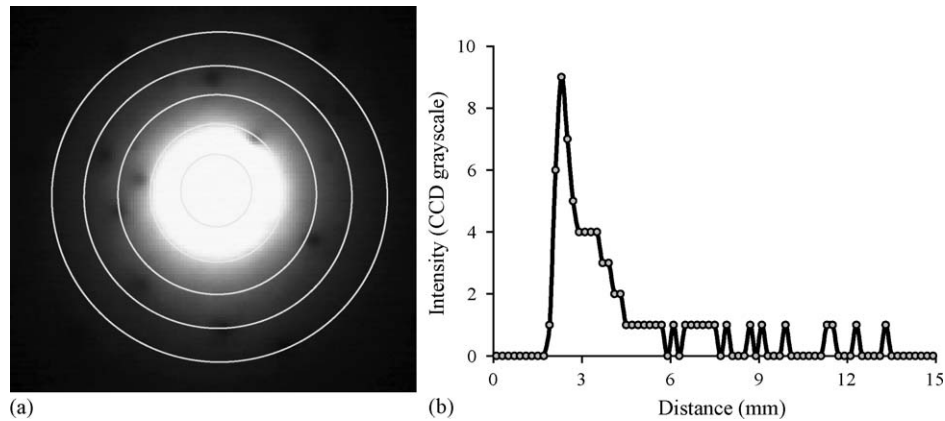


Fig. 3. Removal of noise reflectance (dark spots) from the scattering image of a 'Golden Delicious' apple: (a) a raw scattering image with dark spots; (b) intensity difference in the scattering profile after removing 15% low grayscale pixels.

in Fig. 2(a). A modified Lorentzian distribution (MLD) function was used to describe the scattering profile in two axial directions with the light incident point being the origin of the coordinate system (Peng and Lu, 2006a,b). The MLD function is mathematically expressed by Eq. (1)

$$R = a + \frac{b}{1 + (|z|/c)^d} \quad (1)$$

where  $z$  is the scattering distance (mm);  $R$  denotes the average light intensity of each circular band;  $a$  the asymptotic value of light intensity;  $b$  the estimated maximum value of light intensity at the light incident point;  $c$  the full scattering width at half maximal peak value (FWHM); and  $d$  is related to the slope. A computer program was written for fitting the MLD function to the scattering profiles. Each scattering profile was thus uniquely characterized by the four parameters of the MLD. After MLD parameters were determined for each fruit sample at each wavelength, multi-linear regression (MLR) analysis was performed between the MT firmness and MLD parameters.

### 2.5. Removing abnormal pixels from scattering images

Most apples have small, isolated spots on their skin, whose pigments are distinctly different from the rest of the fruit. The majority of these spots on the fruit occur naturally during their growth and maturation; however, some of these spots could be related to defective tissues. These spots can cause unusually low (dark) and/or high (bright) reflectance on the scattering images. Fig. 3(a) shows a raw scattering image from a GD apple, which had a number of dark spots with much lower reflectance than neighboring pixels. These dark spots lowered or distorted the reflectance intensity in the scattering profile and hence should be removed during radial averaging. A filtering method was proposed to remove pixels of the dark (and/or bright) spots so that the scattering profiles would better reflect the properties of normal tissue. In calculating radial scattering profiles, the pixels of low (and/or high) grayscale values were eliminated from each circular band and the aver-

age grayscale value was calculated for the remaining pixels. The corrected average grayscale values were then used to represent the radial intensity of their corresponding circular band. Fig. 3(b) shows how the scattering profile was changed after removing 15% low grayscale pixels. In this study, the maximum grayscale of scattering images was about 245. This typical example indicated that removing dark spots had a greater effect on the scattering area from 2 to 5 mm, where dramatic intensity changes occurred, and the scattering profile after filtering would have caused the maximum difference of 3.7% ( $=9/245$ ). When no or few dark spots were present in the image, the variation in the grayscale values for all pixels within each circular band was much smaller. As a result, the effect of removing pixels on the scattering profile would be negligible.

On the other hand, bright spots on the fruit would cause higher reflectance than their neighboring pixels, which often occur to RD apples. Fig. 4 shows a raw scattering image from an RD apple, which had both dark and bright spots. The light intensity of the scattering profile would be higher if the bright spots were not removed. Consequently, the filtering method

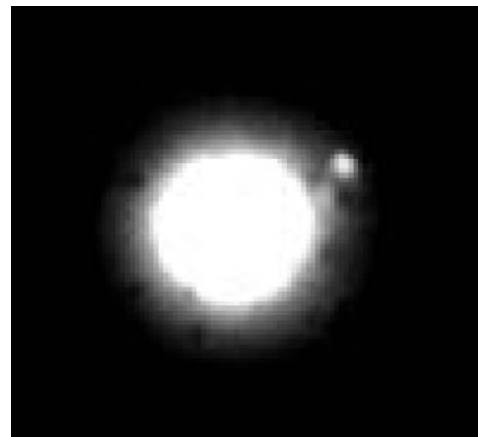


Fig. 4. A raw scattering image of a 'Red Delicious' apple with dark and bright spots.

described above was applied to remove both low and high grayscale pixels in the scattering images.

## 2.6. Correction of scattering images for the fruit shape effect

Apple fruit may be approximated as a sphere. In our previous studies, scattering images acquired from the apples were treated as if they were from a plane and no corrections were made to take into consideration the effect of the fruit surface curvature on the measurement of actual light scattering intensities. Two types of light intensity distortion could occur to the scattering images due to the curved fruit surface; one is the scattering distance distortion and the other is the scattering intensity distortion, both of which are related to the angle  $\theta$  between the imaging direction (vertical) and the surface normal (Fig. 5). In regard to the scattering distance, Fig. 5 shows that the actual scattering distance,  $z$ , for a radial circular band is greater than the horizontal linear distance  $x$ .  $z$  can be calculated from Eq. (2):

$$z = x \tan^{-1} \frac{x}{\sqrt{s^2 - x^2}} \quad (2)$$

where  $s$  is the radius of the apple. In this study, the equatorial diameters of all apple samples were between 69.8 and 82.6 mm; hence we chose the median diameter of 76.2 mm (or  $s = 38.1$  mm) to represent the size of all apples.

In quantifying scattering profiles, ideally we should measure diffuse reflectance in all directions at each point within the scattering area of the fruit, which could not be achieved with the current imaging system. Kienle et al. (1996) performed Monte Carlo simulations to study the angular distribution of diffusely reflected light resulting from a focused beam impinging upon the flat surface of a semi-infinite body. They reported that the patterns of the angular distribution of diffuse reflectance at different locations from the illuminating point were approximately the same; they followed the Lambertian Cosine Law (Kortüm, 1969). The Lambertian Cosine Law should hold for apple fruit since the dimension or radius of the fruit surface is much greater than the photon transfer

mean free path in the fruit. However, corrections of the scattering images would be needed in order to better reflect the scattering profile at the fruit surface. In this study, the scattering images were corrected by taking into consideration the curved surface of the fruit. The following equation was used to calculate the corrected reflectance for a given distance on the surface of the fruit (Fig. 5):

$$R = \frac{R_m}{\cos \theta} = R_m \frac{s}{\sqrt{s^2 - x^2}} \quad (3)$$

By using Eqs. (2) and (3), the plane scattering distance  $x$  and the measured light intensity  $R_m$  of each radial circular band were first converted to the circular scattering distance  $z$  and the corrected reflectance intensity  $R$ . MLD parameters were then determined by fitting the MLD function (Eq. (1)) to the corrected scattering profiles.

## 3. Results and discussion

### 3.1. Light source stability

The light source stability of the improved system was tested by comparing scattering images acquired from a 25-mm thick Teflon disk with and without the light intensity controller that was newly assembled for this research. The light instability was quantified by examining the MLD parameters of the Teflon scattering images. Table 1 shows the variations of MLD parameters at 680 and 880 nm for a period of 1 week. Without the light intensity controller, the changes of MLD parameters ranged between 0.1% and 3.1%, as measured by the coefficient of variation (CV). After the light intensity controller was used, the CV of MLD parameters ranged from 0% to 0.3%. The light source stability improved significantly, as measured by MLD parameters of  $a$ ,  $c$  and  $d$ . Since the parameter  $b$  represents the saturated, peak value, its value changed little for both situations with or without the light intensity controller.

### 3.2. Improvement of scattering images

The percentage of low grayscale pixels removed from the scattering images was increased successively at an interval of 2% from 0% to 30% for RD apple samples. This process resulted in 16 corrected radial scattering profiles for each fruit. For each level of pixel removal, a set of MLD parameters was calculated for all apples. MLR analysis was then performed between MT firmness and MLD parameters at the seven selected wavelengths. The bold curve with solid circle symbols in Fig. 6(a) represents correlation coefficients ( $r$ ) from MLR analysis with different percentages of low grayscale pixels being removed for up to 30%. Firmness predictions improved as the percentage of pixels removed increased from 0% to 18%. The best correlation ( $r = 0.854$ ) was obtained when 18% low grayscale pixels ( $L_p$ ) were removed. Further removal of additional pixels led to a lower

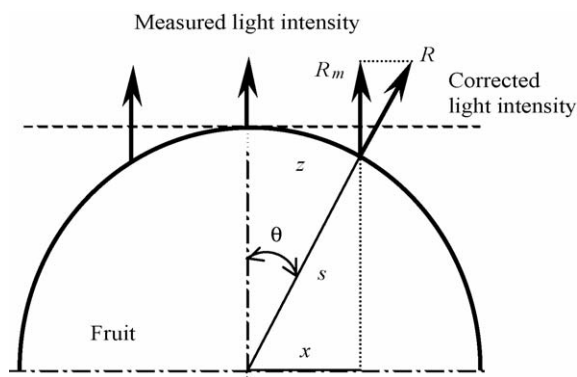


Fig. 5. Conversion of a scattering profile from a spherical dome to a horizontal plane.

Table 1

Statistical analysis results on the stability of the light source without and with the light source controller at two selected wavelengths, as measured by the four parameters ( $a$ ,  $b$ ,  $c$ , and  $d$ ) of the modified Lorentzian distribution (MLD) function for the scattering images acquired from a reference Teflon disk over a 1 week period

	680 nm <sup>a</sup>				880 nm <sup>a</sup>			
	$a$	$b$	$c$	$d$	$a$	$b$	$c$	$d$
Without the light intensity controller								
Mean	3.951	248.315	2.696	5.368	4.678	248.258	3.207	4.791
Standard deviation	0.075	0.217	0.027	0.039	0.145	0.214	0.038	0.119
Coefficient of variation	0.019	0.001	0.010	0.007	0.031	0.001	0.012	0.025
With the light intensity controller								
Mean	3.983	248.518	2.711	5.343	4.666	248.181	3.249	4.763
Standard deviation	0.003	0.142	0.006	0.013	0.015	0.064	0.008	0.011
Coefficient of variation	0.001	0.001	0.002	0.003	0.003	0.000	0.003	0.002

<sup>a</sup> Wavelengths.

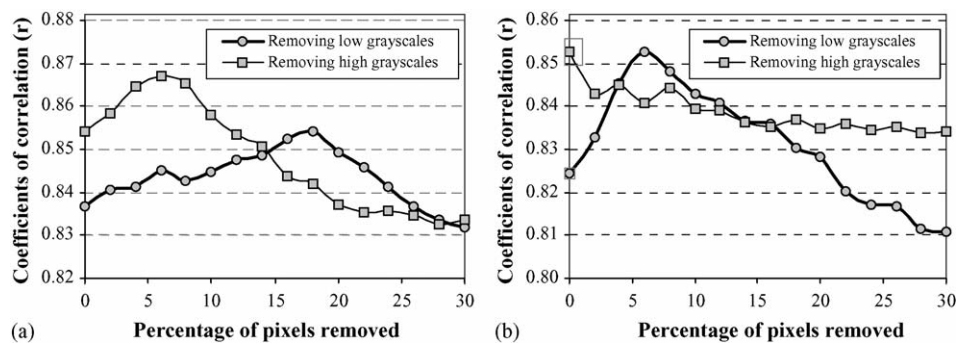


Fig. 6. Distribution of the coefficient of correlation ( $r$ ) with the percentage of filtering low/high grayscale pixels of scattering images for (a) 'Red Delicious' apples; (b) 'Golden Delicious' apples.

correlation. A similar analysis procedure was performed for removing high grayscale pixels under  $L_p = 18\%$ . The thin curve with solid-square symbols in Fig. 6(a) shows a peak after removing high grayscale pixels ( $H_p$ ) of 6% where the  $r$  value was 0.867. Combined with  $L_p = 18\%$  and  $H_p = 6\%$ , the  $r$  value increased to 0.867 from 0.837 which was obtained without pixel removal. Table 2 shows  $r$  values as well as standard errors of estimate (S.E.E.). The correlation coefficient improved by 4% and the S.E.E. by 7% after removing low/high grayscale pixels.

Similarly, the method of removing low and high grayscale pixels was applied to GD apples. Fig. 6(b) shows the change of  $r$  values with the percentage of low and high grayscale pixels being removed. The  $r$  values represent correlations between MT firmness and MLD parameters at the eight

selected wavelengths. These wavelengths are the same as those determined in our previous study (Peng and Lu, 2006a,b). The correlation coefficient had a maximum value of 0.853 after removing 6% low grayscale pixels ( $L_p = 6\%$ ). However, the  $r$  value decreased as high grayscale pixels were removed. This could be due to the fact that GD apples did not have unusually bright spots on their surface. Regression results presented in Table 2 show a 4% improvement in the  $r$  value and 2% in the S.E.E. for GD apples.

### 3.3. Improvement based on apple shape/size

The radial scattering profile was calculated according to scattering distance (Eq. (2)) on the curved surface of apples. MLR analysis was performed between MT firm-

Table 2

Comparison of firmness prediction efficacies from different scattering image improvement methods

Improvement methods	Red Delicious		Golden Delicious	
	$r$	S.E.E.	$r$	S.E.E.
Without improvement	0.837	8.27	0.824	8.14
Filtering low/high grayscale pixels	0.867	7.70	0.853	8.00
Scattering distance conversion based on apple shape	0.854	7.89	0.842	7.60
Light intensity conversion based on apple shape	0.866	7.65	0.850	7.42
With all improvements combined	0.905	6.38	0.898	6.12

Note:  $r$  is the coefficient of correlation; S.E.E. is the standard error of estimate. The unit of S.E.E. is Newtons (N).

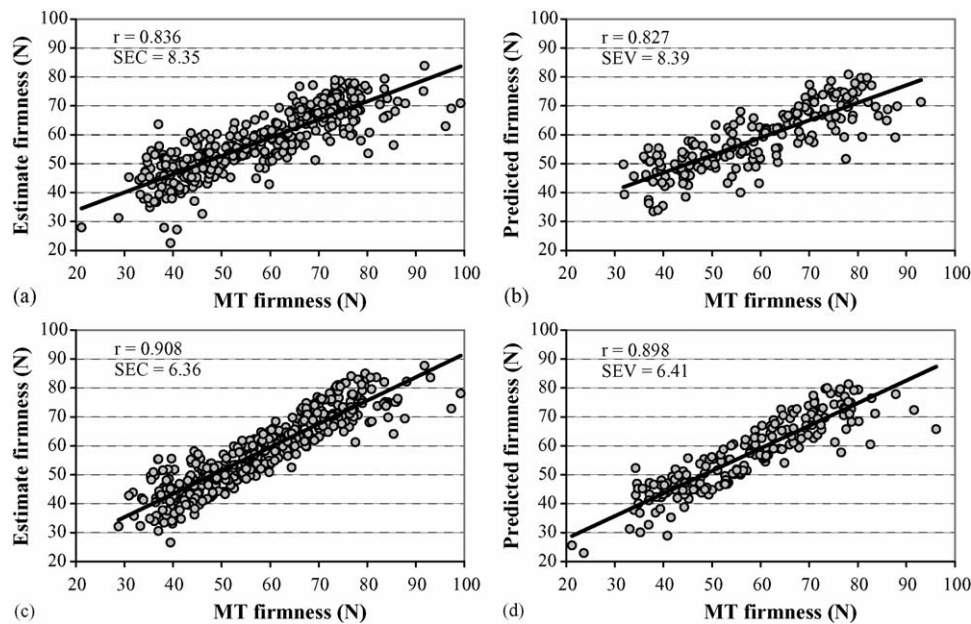


Fig. 7. Correlation between Magness–Taylor (MT) firmness and estimated firmness for ‘Red Delicious’ apples: the results of calibration (a) and validation (b) before scattering profiles were corrected, and the results of calibration (c) and validation (d) after corrections.

ness and MLD parameters for all RD apples at the seven wavelengths mentioned above. The  $r$  value and its corresponding S.E.E. are shown in Table 2. Likewise, regression results for all GD apples are also shown in Table 2. The  $r$  value increased by 0.017 and 0.018 for RD and GD, respectively.

After the scattering intensities were corrected using Eq. (3), the  $r$  value increased by 0.029 and 0.026 for RD and GD apples, respectively (Table 2).

### 3.4. Firmness predictions before and after scattering improvements

Separate model calibrations and validations were performed for the two cultivars of apples. A total of 572 RD apple samples were divided into two groups by the ratio of 2 to 1: 381 apples were used for calibration and the remaining 191 apples for validation. Without any improvements, MT firmness and MLD parameters at the seven wave-

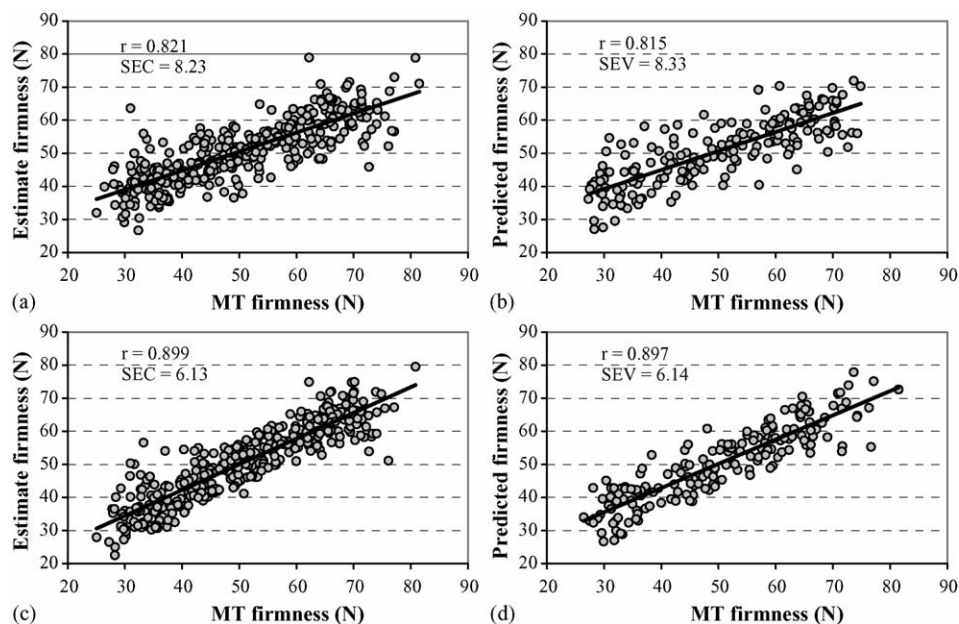


Fig. 8. Correlation between Magness–Taylor (MT) firmness and estimated firmness for ‘Golden Delicious’ apples: the results of calibration (a) and validation (b) before image corrections were made, and the results of calibration (c) and validation (d) after corrections.

lengths were regressed by the MLR analysis for 381 calibration samples, and a prediction model was developed with the  $r$  value of 0.836 and the standard error of calibration (S.E.C.) of 8.35 N (Fig. 7(a)). For the validation samples, the model was able to predict apple firmness with the  $r$  value of 0.827 and the standard error of validation (S.E.V.) of 8.39 N (Fig. 7(b)). These results are comparable to those reported by Peng and Lu (2006a,b). When the scattering images were improved by correcting the light intensity and radial scattering distance and removing low/high grayscale pixels, the new prediction model was obtained with  $r=0.908$  and S.E.C.=6.36 N for calibration samples (Fig. 7(c)), and  $r=0.898$  and S.E.V.=6.41 N for validation samples (Fig. 7(d)). The difference in the  $r$  value between the original prediction model and the improved model was 0.071% or 9% for the validation samples. The image correction methods greatly improved firmness predictions, as measured by S.E.V. (8.39 N versus 6.41 N or 24% improvement).

Similarly, a total of 547 GD apple samples were divided into two groups: 365 apples for calibration and 182 apples for validation. MT firmness and MLD parameters at the eight wavelengths were regressed for the calibration samples without any improvements. Fig. 8(a) and (b) shows results for calibration and validation, respectively. After the image improvement methods were used, a much better prediction model was obtained with  $r=0.899$  and S.E.C.=6.13 N for calibration samples (Fig. 8(c)) and  $r=0.897$  and S.E.V.=6.14 N for validation samples (Fig. 8(d)). The  $r$  value increased by 0.082 (or 10%) and the S.E.V. improved by 26% in comparison with those before the scattering improvement.

#### 4. Discussion

The camera used in this study was a low cost CCD camera with the 8-bit dynamic range and lower photon efficiencies. The actual CCD grayscale ranges from 0 to 245 due to the presence of dark current. This has restricted us from obtaining higher resolution scattering signals, which are critical for firmness predictions. In view of this fact, the firmness prediction results from this study are rather remarkable.

Light scattering profiles are influenced by the shape of apples. Incorporating fruit surface curvature resulted in improved firmness predictions. In this study, all apple samples were considered to be spherical and of the same size. The actual fruit size in the test samples varied between 69.8 and 82.6 mm. Therefore, further improvements in apple firmness prediction may be achieved by measuring and incorporating individual apple's size and/or shape during the acquisition of light scattering images.

Abnormally low and/or high reflectance from small, isolated spots of distinctively different pigments on apples and fruit shape/size negatively affected scattering profiles and thus fruit firmness predictions. Removing low/high grayscale pixels of the scattering images and the correction of light scattering intensity and distance were effective for improv-

ing fruit firmness predictions. In addition, the light intensity controller increased the light source stability considerably. With these improvements, the multispectral imaging system gave much better firmness predictions with  $r=0.898$  and S.E.V.=6.41 N for 'Red Delicious' apples, and  $r=0.897$  and S.E.V.=6.14 N for 'Golden Delicious' apples. The multispectral scattering technique coupled with the modified Lorentzian distribution method provides a practicable means for non-destructive prediction of apple fruit firmness.

#### Acknowledgements

The authors wish to thank Mr. Benjamin Bailey and Mr. Yonggang (Gary) Qin for their technical support in this research.

#### References

- Chen, P., Tjan Y., 1996. A low-mass impact sensor for high-speed firmness sensing of fruits. Ag. Eng.'96—Conference on Agricultural Engineering, Paper 96F-003. Sponsored by CIGR.
- Delwiche, M.J., McDonald, T., Bowers, S.V., 1987. Determination of peach firmness by analysis of impact forces. Trans. ASAE 30, 249–254.
- Delwiche, M.J., Sarig, Y., 1991. A probe impact sensor for fruit firmness measurement. Trans. ASAE 34, 187–192.
- Galili, N., Shmulevich, I., Benichou, N., 1998. Acoustic testing of avocado for fruit ripeness evaluation. Trans. ASAE 41, 399–407.
- Kienle, A., Lilge, L., Patterson, M.S., Hibst, R., Steiner, R., Wilson, B.C., 1996. Spatially resolved absolute diffuse reflectance measurements for non-invasive determination of the optical scattering and absorption coefficients of biological tissue. Appl. Opt. 35, 2304–2314.
- Kortüm, G., 1969. Reflectance Spectroscopy: Principles, Methods, Applications. Springer-Verlag, New York.
- Lu, R., 2003. Near-infrared multispectral scattering for assessing internal quality of apple fruit. SPIE Proc. 5271, 313–320.
- Lu, R., 2004. Multispectral imaging for predicting firmness and soluble solids content of apple fruit. Postharvest Biol. Technol. 31, 147–157.
- Lu, R., Ariana, D., 2002. A near-infrared sensing technique for measuring internal quality of apple fruit. Appl. Eng. Agric. 18, 585–590.
- Lu, R., Guyer, D.E., Beaudry, R.M., 2000. Determination of firmness and sugar content of apples using near-infrared diffuse reflectance. J. Texture Stud. 31, 615–630.
- McGlone, V.A., Abe, H., Kawano, S., 1997. Kiwifruit firmness by near infrared light scattering. J. Near Infrared Spec. 5, 83–89.
- McGlone, V.A., Kawano, S., 1998. Firmness, dry-matter and soluble-solids assessment of postharvest kiwifruit by NIR spectroscopy. Postharvest Biol. Technol. 13, 131–141.
- McGlone, V.A., Ko, S.M.W., Jordan, R.B., 1999. Non-contact fruit firmness measurement by the laser air-puff method. Trans. ASAE 45, 1391–1397.
- Meredith, F.I., Leffler, R.G., Lyon, C.E., 1990. Detection of firmness in peaches by impact force response. Trans. ASAE 33, 186–188.
- Ozer, F., Engel, B.A., Simon, J.E., 1998. A multiple impact approach non-destructive measurement of fruit firmness and maturity. Trans. ASAE 41, 871–876.
- Peng, Y., Lu, R., 2005. Modeling multispectral scattering profiles for prediction of apple fruit firmness. Trans. ASAE 48, 235–242.
- Peng, Y., Lu, R., 2006a. An LCTF-based multispectral imaging system for estimation of apple fruit firmness: Part I. Acquisition and characterization of scattering images. Trans. ASAE 49, 259–267.

- Peng, Y., Lu, R., 2006b. An LCTF-based multispectral imaging system for estimation of apple fruit firmness: Part II. Selection of optimal wavelengths and development of prediction models. *Trans. ASAE* 49, 269–275.
- Ruiz-Altisent, M., Ortiz-Canavate, J., 2005. Instrumentation and procedures for commercial non-destructive determination of firmness of various fruits. ASAE Paper No. 056176. St. Joseph, MI.
- Shmulevich, I., Galili, N., Howarth, M.S., 2003. Non-destructive dynamic testing of apples for firmness evaluation. *Postharvest Biol. Technol.* 29, 287–299.
- Stone, M.L., Armstrong, P.R., Chen, D.D., Brusewitz, G.H., Maness, N.O., 1998. Peach firmness prediction by multiple location impulse testing. *Trans. ASAE* 41, 115–119.
- Sugiyama, J., Katsurai, T., Hong, J., Koyama, H., Mikuriya, K., 1998. Melon ripeness monitoring by a portable firmness tester. *Trans. ASAE* 41, 121–127.
- Weeks Jr., A.R., 1996. Fundamentals of electronic image processing. *SPIE IEEE Proc.*, 359–360.
- Zhang, X., Stone, M.L., Chen, D., Maness, N.O., Brusewitz, G.H., 1994. Peach firmness determination by puncture resistance, drop impact, and sonic impulse. *Trans. ASAE* 37, 495–500.